The TDUSW Distribution: Properties, Statistical Inference, and Applications to COVID-19 Mortality Data from Two Different Countries

FATHY H. RIAD[1,2], HAMDY M. BARAKAT[1,2], AMR RADWAN[1,3]
[1]Department of Mathematics, College of Science
Jouf University, P.O. Box 2014, Sakaka
SAUDI ARABIA

[2]Department of Mathematics, Faculty of Science
Minia University, Minia 61519
EGYPT

[3]Department of Mathematics, Faculty of Science
Sohag University, Sohag 82524
EGYPT

Abstract: The proposed TDUSW distribution provides a flexible framework for modeling lifetime and reliability data, accommodating various distributional shapes, including skewed and heavy-tailed patterns. Its main statistical properties, including the cumulative distribution function, probability density function, hazard rate function, quantile function, and moments, are derived. Six estimation methods are investigated: maximum likelihood, least squares, weighted least squares, maximum product of spacings, Cramér–von Mises, and Anderson–Darling. A Monte Carlo simulation study evaluates their performance under different parameter settings and sample sizes. Furthermore, two real-world COVID-19 mortality datasets from Canada and the United Kingdom are analyzed to assess the proposed model's practical applicability. The results demonstrate that estimation accuracy generally improves with increasing sample size. Moreover, the TDUSW distribution provides a competitive and satisfactory fit to both datasets compared with several established lifetime distributions, highlighting its potential for modeling mortality and reliability data.

Key-Words: TDUSW distribution; COVID-19 mortality rate; lifetime distributions; maximum likelihood estimation; simulation study; hazard rate function.

Received: March 9, 2026. Revised: July 13, 2026. Accepted: August 11, 2026. Available online: November 25, 2026.

1 Introduction

Probability distributions provide fundamental tools for describing uncertainty and interpreting data in a wide range of disciplines, including reliability engineering, survival analysis, medicine, and applied statistics [1], [2]. However, empirical observations may display pronounced asymmetry, heavy tails, or diverse hazard rate patterns that are not adequately captured by conventional lifetime models [3]. This limitation has encouraged the development of more adaptable distributions that can represent heterogeneous data structures and improve the quality of statistical modeling [4], [5].

The Weibull distribution is a well-established model for lifetime analysis because of its tractable mathematical form and its usefulness in reliability and survival applications [6]. Despite these advantages, its conventional formulation may be inadequate when the observed data exhibit complex tail characteristics or hazard rate patterns beyond those it can represent [7]. Various extensions and transformations of the Weibull distribution have therefore been investigated to overcome these restrictions [8], [9]. More generally, generator-based approaches offer a systematic means of constructing new distributions from established probability models, allowing a broader range of distributional and hazard rate shapes [10], [11]. Representative examples include the exponentiated, Kumaraswamy-generated, Topp–Leone-generated, and trigonometric-generated families [12], [13]. These approaches have found applications in several fields, including reliability engineering, environmental research, biological studies, and medical sciences [14], [15].

The analysis of COVID-19 data has further highlighted the importance of selecting probability distributions that adequately describe mortality patterns and related epidemiological observations [16], [17]. Such data may exhibit substantial variation and asymmetric behavior, making flexible statistical models particularly useful for parameter estimation and goodness-of-fit assessment [18]. Accordingly, a variety of generalized probability distributions have been employed to investigate COVID-19 mortality observations collected from different geographical regions [19], [20]. These applications provide a practical setting in which the adequacy of newly developed statistical models can be evaluated.

In this context, the present study proposes the TDUSW distribution as an alternative two-parameter lifetime model. Let X be a nonnegative random variable following the proposed distribution, where

$\alpha > 0$ and $\beta > 0$. Its cumulative distribution function (CDF) is defined as

$$F(x) = \tan\left[\frac{\pi}{4}\left(\frac{e^{1-e^{-\beta x^{\alpha}}}-1}{e-1}\right)\right], x > 0, \alpha, \beta > 0. \quad (1)$$

The corresponding probability density function (PDF) is expressed as

$$f(x) = \frac{\pi\alpha\beta}{4(e-1)} x^{\alpha-1} \exp\left(1 - \beta x^{\alpha} - e^{-\beta x^{\alpha}}\right) \times \sec^2\left[\frac{\pi}{4}\left(\frac{e^{1-e^{-\beta x^{\alpha}}}-1}{e-1}\right)\right], \quad x > 0, \alpha, \beta > 0. \quad (2)$$

The proposed model is investigated through its principal distributional characteristics, including the survival and hazard rate functions, quantile function, and moments. Parameter estimation is examined using several statistical procedures, with maximum likelihood estimation and numerical optimization forming part of the inferential framework [21]. In addition, a Monte Carlo experiment is designed to assess the finite-sample performance of the estimators under different parameter configurations and sample sizes. The empirical relevance of the model is subsequently examined using two COVID-19 mortality data sets, with its goodness-of-fit performance compared against that of established competing distributions [22]. These analyses provide complementary evidence concerning the model's estimation properties and its applicability to observed lifetime data.

Beyond the present investigation, recent developments in dependence modeling suggest opportunities to extend the proposed distribution to multivariate settings. In particular, copula-based constructions have been investigated in related studies to describe dependence structures between random variables [23], [24], [25]. Building on these contributions, a bivariate extension of the TDUSW distribution could be developed to accommodate dependent observations. Further research could also examine the model under censoring schemes, thereby extending its potential applications to survival analysis and reliability studies involving incomplete lifetime information.

The remainder of this paper is organized as follows. Section 2 presents the mathematical properties of the TDUSW distribution. Section 3 describes the estimation procedures for its unknown parameters. Section 4 reports the results of the Monte Carlo simulation study. Section 5 examines two applications involving COVID-19 mortality data. Finally, the main findings and possible directions for further research are summarized in the concluding section.

2 TDUSW Distribution

Using the Weibull baseline model with shape parameters α and β, In this work, the TDUSW distribution is proposed as a new and flexible model for lifetime data analysis. The proposed model is obtained through a trigonometric transformation applied to the Weibull distribution. For $X \geq 0$, inserting the Weibull cumulative distribution function into the proposed generating mechanism leads to the following CDF for the TDUSW distribution:

$$F(x;\Psi) = \tan\left[\frac{\pi}{4}\left(\frac{e^{1-e^{-\beta x^{\alpha}}}-1}{e-1}\right)\right], \quad x > 0,\ \alpha, \beta > 0. \quad (3)$$

In this formulation, $\Psi = (\alpha, \beta)$ specifies the vector of model parameters. The PDF of the TDUSW distribution is subsequently derived by taking the first derivative of Equation (3) with respect to x, resulting in

$$f(x;\Psi) = \frac{\pi\alpha\beta}{4(e-1)} x^{\alpha-1} \exp\left(1 - \beta x^{\alpha} - e^{-\beta x^{\alpha}}\right) \times \sec^2\left[\frac{\pi}{4}\left(\frac{e^{1-e^{-\beta x^{\alpha}}}-1}{e-1}\right)\right], \quad x > 0,\ \alpha, \beta > 0. \quad (4)$$

The hazard rate function of the proposed TDUSW model takes the following form:

$$h(x;\Psi) = \frac{\pi\alpha\beta}{4(e-1)} x^{\alpha-1} \exp\left(1 - \beta x^{\alpha} - e^{-\beta x^{\alpha}}\right) \times \frac{\sec^2\left[\frac{\pi}{4}\left(\frac{e^{1-e^{-\beta x^{\alpha}}}-1}{e-1}\right)\right]}{1 - \tan\left[\frac{\pi}{4}\left(\frac{e^{1-e^{-\beta x^{\alpha}}}-1}{e-1}\right)\right]}, \quad x > 0,\ \alpha, \beta > 0. \quad (5)$$

The graphical behavior of the TDUSW distribution indicates that the proposed model possesses high flexibility in modeling lifetime observations. The resulting characteristics are determined by the particular values assigned to α and β , the density function may exhibit different right-skewed and unimodal shapes. Moreover, the hazard rate function can accommodate increasing, decreasing, and bathtub-shaped failure rates.

An important advantage of the TDUSW distribution over the classical Weibull model is its ability to provide better fitting performance for data sets with complex hazard structures. Therefore, the proposed model can be considered a useful alternative for analyzing lifetime, reliability, and survival data in engineering and medical applications.

3 Statistical Properties of the TDUSW Distribution

3.1 Linear Expansion of the TDUSW Distribution

In this subsection, a series expansion form of the TDUSW distribution is introduced. This representation is useful for deriving several distributional properties in a simpler way.

Using the generalized power series expansion, the probability density function of the TDUSW distribution can be expressed as

$$f(x;\Theta) = \sum_{j=0}^{\infty} \frac{(-1)^j}{j!}\, c_j\, g(x;\beta) \times [G(x;\beta)]^{\alpha(j+1)-1} [1-G(x;\beta)]^{\alpha(j+1)+1}. \quad (6)$$

where $g(x;\beta)$ and $G(x;\beta)$ denote the baseline density and cumulative distribution functions, respectively, and c_j are constants depending on the parameter vector Θ.

Accordingly, the TDUSW density can be rewritten in the following linear mixture form:

$$f(x;\Theta) = \sum_{j,k,h=0}^{\infty} \omega_{j,k,h}\, (\beta(h+1)) x^{\beta(h+1)-1} e^{-x^{\beta(h+1)}}, \quad (7)$$

where

$$\omega_{j,k,h} = \frac{\alpha(-1)^{j+k+h}}{(h+1)j!} \times \binom{\alpha(j+1)+k}{k} \binom{\alpha(j+1)+k-1}{h}.$$

As a consequence, the density of the TDUSW distribution may be expressed through an infinite series of weighted Weibull-type components characterized by the shape parameter $\beta(h+1)$. This form is particularly useful for deriving several distributional quantities, including moments, generating functions, and other relevant statistical properties.

3.2 Quantile Function of the TDUSW Distribution

The quantile function plays an important role in random sample generation and descriptive statistical analysis. The quantile function of the TDUSW distribution can be obtained by inverting the cumulative distribution function given in Equation (3). Let $0 < q < 1$, then the quantile function is obtained as

$$x_q = \left[-\frac{1}{\beta} \ln \left\{ 1 - \ln \left[1 + \frac{4(e-1)}{\pi} \tan^{-1}(q) \right] \right\} \right]^{1/\alpha}. \quad (8)$$

In particular, the quartiles of the TDUSW distribution can be determined by substituting $q = 0.25, 0.50$, and 0.75 into Equation (8).

3.3 Moments of the TDUSW Distribution

Several key features of the TDUSW distribution can be characterized through its moments. These include the mean, variance, skewness, and kurtosis, which describe different aspects of the distributional shape. The rth-order non-central moment of X is given by

$$\mu'_r = E(X^r) = \int_0^{\infty} x^r f(x;\Psi)\, dx. \quad (9)$$

Substituting Equation (7) into Equation (9), the rth moment can be expressed as

$$\mu'_r = \sum_{m=0}^{\infty} \omega_m \int_0^{\infty} x^r g(x;\alpha,\beta) \left[G(x;\alpha,\beta)\right]^m dx. \quad (10)$$

After simplification, the rth moment may be represented in terms of the gamma function as

$$\mu'_r = \sum_{m=0}^{\infty} \omega_m \frac{\Gamma\left(1+\frac{r}{\alpha}\right)}{\beta^{\,r/\alpha}}. \quad (11)$$

In a similar manner, the rth-order incomplete moment can be expressed in the following form:

$$\varphi_r(t) = \int_0^t x^r f(x;\Psi)\, dx, \qquad t > 0.$$

$$\varphi_r(t) = \sum_{m=0}^{\infty} \omega_m \int_0^t x^r g(x;\alpha,\beta) \left[G(x;\alpha,\beta)\right]^m dx.$$

$$\varphi_r(t) = \sum_{m=0}^{\infty} \sum_{k=0}^{m} \omega_m (-1)^k \binom{m}{k} \frac{\gamma\left(1+\frac{r}{\alpha}, (k+1)\beta t^{\alpha}\right)}{[(k+1)\beta]^{r/\alpha}} \quad (12)$$

where

$$\gamma(s,x) = \int_0^x u^{s-1} e^{-u} du$$

denotes the lower incomplete gamma function. The incomplete moments are useful in reliability analysis, mean residual life studies, and income inequality measures.

4 Methods of Estimation

This section considers several inferential approaches for obtaining estimates of the unknown parameters in the TDUSW model. Let $X_1, X_2, \ldots, X_n$ represent a random sample of n observations from the TDUSW distribution, whose parameter vector is denoted by $\Psi = (\alpha, \beta)$. Several estimation techniques can be employed to estimate the model parameters, including the maximum likelihood estimators (MLEs), least-squares estimators (LSEs), weighted least-squares estimators (WLSEs), maximum

product spacing estimators (MPSEs), Cramér–von Mises estimators (CVMEs), and Anderson–Darling estimators (ADEs).

4.1 Maximum Likelihood Estimation

Suppose that $x_1, x_2, \ldots, x_n$ is a random sample from the TDUSW distribution. Using the probability density function given in Equation (4), the likelihood function can be written as

$$L(\Psi) = \prod_{i=1}^{n} f(x_i; \Psi).$$

Hence, the likelihood function becomes

$$\begin{aligned} L(\Psi) = & \left[\frac{\pi\alpha\beta}{4(e-1)}\right]^n \prod_{i=1}^{n} x_i^{\alpha-1} \\ & \times \exp\left(1 - \beta x_i^{\alpha} - e^{-\beta x_i^{\alpha}}\right) \\ & \times \sec^2\left[\frac{\pi}{4}\left(\frac{e^{1-e^{-\beta x_i^{\alpha}}} - 1}{e-1}\right)\right]. \end{aligned} \tag{13}$$

Taking the natural logarithm of Equation (13), the log-likelihood function is obtained as

$$\begin{aligned} \ell(\Psi) = & \, n \ln\left(\frac{\pi}{4(e-1)}\right) + n\ln(\alpha) + n\ln(\beta) \\ & + (\alpha - 1)\sum_{i=1}^{n} \ln(x_i) \\ & + \sum_{i=1}^{n}\left(1 - \beta x_i^{\alpha} - e^{-\beta x_i^{\alpha}}\right) \\ & + 2\sum_{i=1}^{n} \ln\left[\sec\left(\frac{\pi}{4}\left(\frac{e^{1-e^{-\beta x_i^{\alpha}}} - 1}{e-1}\right)\right)\right]. \end{aligned} \tag{14}$$

To determine the maximum likelihood estimates of α and β, Equation (13) is differentiated with respect to each unknown parameter, and the resulting score equations are set equal to zero.

The score function corresponding to the parameter α, obtained from the first derivative of the log-likelihood function, is given by

$$\begin{aligned} \frac{\partial \ell(\Psi)}{\partial \alpha} = & \frac{n}{\alpha} + \sum_{i=1}^{n} \log(x_i) - \beta \sum_{i=1}^{n} x_i^{\alpha} \log(x_i) \\ & + \beta \sum_{i=1}^{n} x_i^{\alpha} e^{-\beta x_i^{\alpha}} \log(x_i) + R_1(\alpha, \beta). \end{aligned} \tag{15}$$

where $R_1(\alpha, \beta)$ represents the derivative term associated with the trigonometric component.

Similarly, the derivative with respect to β is obtained as

$$\frac{\partial \ell(\Psi)}{\partial \beta} = \frac{n}{\beta} - \sum_{i=1}^{n} x_i^{\alpha} + \sum_{i=1}^{n} x_i^{\alpha} e^{-\beta x_i^{\alpha}} + R_2(\alpha, \beta), \tag{16}$$

where $R_2(\alpha, \beta)$ denotes the derivative corresponding to the secant function term.

Since Equations (15) and (16) cannot be solved analytically, numerical iterative techniques are required to obtain the maximum likelihood estimates of the parameters. The Newton–Raphson algorithm can be implemented using statistical software such as `R` to determine the parameter estimates numerically.

4.2 Least Squares and Weighted Least Squares Estimation

In this subsection, the least squares and weighted least squares estimation methods are considered for estimating the parameters of the TDUSW distribution. These approaches are commonly used in statistical inference because of their computational simplicity and good estimation performance for continuous distributions.

Suppose that $x_{(1)} < x_{(2)} < \cdots < x_{(n)}$ are the ordered observations arising from the TDUSW distribution, where $\Psi = (\alpha, \beta)$ denotes its parameter vector. Under the least-squares and weighted least-squares frameworks, the unknown parameters are estimated by optimizing the criterion given below:

$$V(\Psi) = \sum_{i=1}^{n} w_i \left[F(x_{(i)}; \Psi) - \frac{i}{n+1}\right]^2, \tag{17}$$

where $F(x_{(i)}; \Psi)$ is the cumulative distribution function of the TDUSW distribution given by

$$F(x_{(i)}; \Psi) = \tan\left[\frac{\pi}{4}\left(\frac{e^{\,1-e^{-\beta x_{(i)}^{\alpha}}} - 1}{e-1}\right)\right].$$

For the ordinary least squares method, the weights are taken as

$$w_i = 1,$$

Under the weighted least-squares procedure, the weighting factors are specified according to the following expression:

$$w_i = \frac{(n+1)^2(n+2)}{i(n-i+1)}.$$

Substituting the TDUSW cumulative distribution function into Equation (17), the objective function becomes

$$V(\Psi) = \sum_{i=1}^{n} w_i \left[\tan\left(\frac{\pi}{4} \left(\frac{e^{1-e^{-\beta x_{(i)}^{\alpha}}} - 1}{e-1} \right) \right) - \frac{i}{n+1} \right]^2. \quad (18)$$

For the least-squares and weighted least-squares approaches, the unknown parameters are obtained by setting the partial derivatives of Equation (18) with respect to α and β equal to zero and solving the resulting nonlinear system numerically.

In particular, differentiation of $V(\Psi)$ with respect to α gives

$$\frac{\partial V(\Psi)}{\partial \alpha} = 2 \sum_{i=1}^{n} w_i \left[F(x_{(i)}; \Psi) - \frac{i}{n+1} \right] \times \frac{\partial F(x_{(i)}; \Psi)}{\partial \alpha}, \quad (19)$$

where

$$\frac{\partial F(x_{(i)}; \Psi)}{\partial \alpha} = \frac{\pi}{4(e-1)} \sec^2 \left[\frac{\pi}{4} \left(\frac{e^{1-e^{-\beta x_{(i)}^{\alpha}}} - 1}{e-1} \right) \right] \times e^{1-e^{-\beta x_{(i)}^{\alpha}}} e^{-\beta x_{(i)}^{\alpha}} \beta x_{(i)}^{\alpha} \log(x_{(i)}).$$

Similarly, the derivative with respect to β is obtained as

$$\frac{\partial V(\Psi)}{\partial \beta} = 2 \sum_{i=1}^{n} w_i \left[F(x_{(i)}; \Psi) - \frac{i}{n+1} \right] \times \frac{\partial F(x_{(i)}; \Psi)}{\partial \beta}, \quad (20)$$

where

$$\frac{\partial F(x_{(i)}; \Psi)}{\partial \alpha} = \frac{\pi \beta}{4(e-1)} x_{(i)}^{\alpha} \ln(x_{(i)}) \times \exp\left(1 - \beta x_{(i)}^{\alpha} - e^{-\beta x_{(i)}^{\alpha}}\right) \times \sec^2 \left[\frac{\pi}{4} \left(\frac{e^{1-e^{-\beta x_{(i)}^{\alpha}}} - 1}{e-1} \right) \right]$$

Because Equations (19) and (20) are nonlinear, numerical optimization methods are required to compute the least squares and weighted least squares estimates. Statistical software such as R may be used to obtain the estimates iteratively.

4.3 Estimation via the Maximum Product of Spacings Method

In this subsection, the maximum product of spacings (MPS) method is considered as an alternative estimation procedure to the maximum likelihood approach. The MPS technique is widely used for estimating the parameters of continuous probability distributions because of its good numerical stability and efficiency in many practical applications.

Let

$$x_{(1)} < x_{(2)} < \cdots < x_{(n)}$$

be the ordered random sample obtained from the TDUSW distribution with parameter vector $\Psi = (\alpha, \beta)$. The uniform spacings are defined as

$$D_i(\Psi) = F(x_{(i)}; \Psi) - F(x_{(i-1)}; \Psi), i = 1, 2, \ldots, n+1, \quad (21)$$

where

$$F(x_{(0)}; \Psi) = 0, \qquad F(x_{(n+1)}; \Psi) = 1,$$

and

$$\sum_{i=1}^{n+1} D_i(\Psi) = 1.$$

Substitution of the TDUSW cumulative distribution function into the spacing formulation yields the following expression:

$$D_i(\Psi) = \tan\left[\frac{\pi}{4} \left(\frac{e^{1-e^{-\beta x_{(i)}^{\alpha}}} - 1}{e-1} \right) \right] - \tan\left[\frac{\pi}{4} \left(\frac{e^{1-e^{-\beta x_{(i-1)}^{\alpha}}} - 1}{e-1} \right) \right]. \quad (22)$$

The geometric mean of the spacings is obtained by maximizing the following objective function

$$G(\Psi) = \frac{1}{n+1} \sum_{i=1}^{n+1} \log\left[D_i(\Psi) \right]. \quad (23)$$

Substituting Equation (22) into Equation (23), we obtain

$$G(\Psi) = \frac{1}{n+1} \sum_{i=1}^{n+1} \log\left\{ \tan\left[\frac{\pi}{4} \left(\frac{e^{1-e^{-\beta x_{(i)}^{\alpha}}} - 1}{e-1} \right) \right] - \tan\left[\frac{\pi}{4} \left(\frac{e^{1-e^{-\beta x_{(i-1)}^{\alpha}}} - 1}{e-1} \right) \right] \right\}. \quad (24)$$

Within the maximum product-of-spacings framework, the unknown parameters α and β

are estimated by maximizing the criterion defined in Equation (24). The score equation associated with α is obtained from the first partial derivative of $G(\Psi)$, which is given by

$$\frac{\partial G(\Psi)}{\partial \alpha} = \frac{1}{n+1}\sum_{i=1}^{n+1}\frac{\frac{\partial D_i(\Psi)}{\partial \alpha}}{D_i(\Psi)}, \tag{25}$$

where

$$\frac{\partial D_i(\Psi)}{\partial \alpha} = \frac{\partial F(x_{(i)};\Psi)}{\partial \alpha} - \frac{\partial F(x_{(i-1)};\Psi)}{\partial \alpha}.$$

Similarly, the derivative with respect to β is obtained as

$$\frac{\partial G(\Psi)}{\partial \beta} = \frac{1}{n+1}\sum_{i=1}^{n+1}\frac{\frac{\partial D_i(\Psi)}{\partial \beta}}{D_i(\Psi)}. \tag{26}$$

Because the resulting equations are nonlinear, numerical iterative methods are required to determine the MPSEs of the model parameters. Statistical software such as R can be employed to solve Equations (25) and (26) numerically.

4.4 Cramér–von Mises Estimation

The parameter estimation procedure based on the Cramér–von Mises method seeks the parameter values that provide the closest agreement between the empirical distribution and the theoretical CDF. This criterion belongs to the class of minimum-distance methods commonly employed for continuous probability distributions. Let $x_{(1)} < x_{(2)} < \cdots < x_{(n)}$ be the ordered sample observations from the TDUSW distribution, with $\Psi = (\alpha, \beta)$ denoting its unknown parameter vector. The corresponding objective function can be expressed as

$$C(\Psi) = \frac{1}{12n} + \sum_{i=1}^{n}\left[F(x_{(i)};\Psi) - \frac{2i-1}{2n}\right]^2, \tag{27}$$

where $F(x_{(i)};\Psi)$ denotes the cumulative distribution function of the TDUSW distribution.

Substituting the TDUSW cumulative distribution function into Equation (27), we obtain

$$C(\Psi) = \frac{1}{12n} + \sum_{i=1}^{n}\left[\tan\left(\frac{\pi}{4}\left(\frac{e^{1-e^{-\beta x_{(i)}^{\alpha}}}-1}{e-1}\right)\right) - \frac{2i-1}{2n}\right]^2. \tag{28}$$

Within the Cramér–von Mises framework, the unknown parameters α and β are estimated by seeking the values that minimize the objective function given in Equation (28). The derivative of $C(\Psi)$ with respect to α is given by

$$\frac{\partial C(\Psi)}{\partial \alpha} = 2\sum_{i=1}^{n}\left[F(x_{(i)};\Psi) - \frac{2i-1}{2n}\right]\frac{\partial F(x_{(i)};\Psi)}{\partial \alpha}, \tag{29}$$

while the derivative with respect to β becomes

$$\frac{\partial C(\Psi)}{\partial \beta} = 2\sum_{i=1}^{n}\left[F(x_{(i)};\Psi) - \frac{2i-1}{2n}\right]\frac{\partial F(x_{(i)};\Psi)}{\partial \beta}. \tag{30}$$

Because the resulting equations are nonlinear, numerical optimization procedures are required to obtain the CVM estimates.

4.5 Anderson–Darling Estimation

The Anderson–Darling method is a tail-sensitive minimum-distance approach that gives greater importance to differences between the fitted and empirical distributions in the extreme regions. Consequently, it can provide an effective estimation strategy when the observed sample contains unusually large or small values or exhibits substantial tail heaviness. The Anderson–Darling objective function for the TDUSW distribution is defined as

$$A(\Psi) = -n - \frac{1}{n}\sum_{i=1}^{n}(2i-1)\Big[\log F(x_{(i)};\Psi) + \log\left(1 - F(x_{(n+1-i)};\Psi)\right)\Big]. \tag{31}$$

Using the cumulative distribution function of the TDUSW distribution, Equation (31) can be rewritten as

$$A(\Psi) = -n - \frac{1}{n}\sum_{i=1}^{n}(2i-1) \times \left[\ln\left(\tan\left[\frac{\pi}{4}\left(\frac{e^{1-e^{-\beta x_{(i)}^{\alpha}}}-1}{e-1}\right)\right]\right) + \ln\left(1 - \tan\left[\frac{\pi}{4}\left(\frac{e^{1-e^{-\beta x_{(n+1-i)}^{\alpha}}}-1}{e-1}\right)\right]\right)\right]. \tag{32}$$

The Anderson–Darling estimators (ADEs) of the TDUSW parameters are obtained by minimizing Equation (32) with respect to α and β. Since the objective function does not admit explicit analytical solutions, iterative numerical methods are used to compute the parameter estimates.

5 Simulation Results

Under the Cramér–von Mises estimation scheme, the parameter vector $\Psi = (\alpha, \beta)$ is determined

by minimizing the criterion defined in Equation (28).estimation methods for the TDUSW distribution parameters. The simulation study compares the behavior of six parameter estimation methods, namely MLE, LSE, WLSE, MPSE, CVME, and ADE, representing maximum likelihood, least squares, weighted least squares, maximum product of spacings, Cramér–von Mises, and Anderson–Darling estimation, respectively.

The simulation experiment is performed for several combinations of the parameter values

$$\alpha = (0.6,\ 1.7,\ 3) \qquad \text{and} \qquad \beta = (0.6,\ 1.7,\ 3),$$

A Monte Carlo study is performed with sample sizes $n = 25,\ 70,$ and 150. For each combination of the model parameters, $10{,}000$ simulated samples are produced from the TDUSW model by means of the quantile function in Equation (8). The unknown parameters are estimated separately by each of the six methods for every generated sample. Their estimation accuracy is subsequently compared in terms of the mean of the obtained estimates and the corresponding mean squared error (MSE), where the latter is defined by

$$\mathrm{MSE}(\widehat{\theta}) = \frac{1}{N}\sum_{j=1}^{N}\left(\widehat{\theta}_j - \theta\right)^2, \qquad (33)$$

In this notation, $\hat{\theta}_j$ is the estimated value of the parameter from replication j, while θ indicates its actual value. The simulation study and all numerical computations are implemented in the R software environment. The simulation findings are summarized in Table 1 (Appendix), Table 2 (Appendix), and Table 3 (Appendix). In general, the results indicate that the mean estimates produced by all estimation methods gradually approach the true parameter values as the sample size increases. Moreover, an increase in the sample size is accompanied by a reduction in the corresponding MSE values, which supports the consistency of the proposed estimation procedures. Moreover, the simulation study suggests that the MLE and MPSE approaches usually provide smaller MSE values compared with the other estimation procedures in most parameter settings. Therefore, these methods can be considered more efficient for estimating the parameters of the TDUSW distribution.

5.1 Concluding Remarks on the Simulation Study

Based on the simulation results reported in Table 1 (Appendix), Table 2 (Appendix), and Table 3 (Appendix),

the following conclusions can be drawn:

1. The estimated means are generally close to the true values for the different choices of α and β, confirming the satisfactory behavior of the considered estimators.
2. AThe simulation results reveal a clear tendency for the MSE to decrease as n increases from 25 to 150, suggesting that the estimators become progressively more accurate with larger sample sizes.
3. The MPS estimator achieves relatively small MSE values in many settings, whereas MLE, LS, WLS, CVM, and AD also provide competitive results.
4. For larger samples, the differences among the estimation methods are generally reduced, indicating greater stability of the estimates.
5. Taken as a whole, the numerical results demonstrate that the six considered methods perform adequately in estimating the parameters of the TDUSW model.

6 Application to Real Data Sets

The practical applicability of the TDUSW distribution is illustrated using a real data set and by comparing its performance with several established lifetime models, including the inverse Weibull (IW), inverse exponential (IE), inverse Rayleigh (IR), and Marshall–Olkin exponential (MOEx) distributions. Model adequacy is evaluated using the Kolmogorov–Smirnov (KS) statistic and its p-value, the Anderson–Darling statistic (A^*), and the Cramér–von Mises statistic (W^*). The MLEs of the model parameters and their corresponding standard errors (SEs) are also reported. A model is considered to provide a better fit when it has smaller KS, A^*, and W^* values together with a larger p-value.

6.1 Application 1

The first empirical data set contains 36 consecutive daily observations of COVID-19 mortality in Canada, covering the period between April 10 and May 15, 2020. These observations were retrieved from the World Health Organization database at https://covid19.who.int/. The recorded mortality rates are presented as follows:

3.1091, 3.3825, 3.1444, 3.2135, 2.4946, 3.5146,
4.9274, 3.3769, 6.8686, 3.0914, 4.9378, 3.1091,
3.2823, 3.8594, 4.0480, 4.1685, 3.6426, 3.2110,
2.8636, 3.2218, 2.9078, 3.6346, 2.7957, 4.2781,
4.2202, 1.5157, 2.6029, 3.3592, 2.8349, 3.1348,
2.5261, 1.5806, 2.7704, 2.1901, 2.4141, 1.9048.

The comparative fitting results—comprising estimated parameters, standard errors, and goodness-of-fit measures—are summarized in Table 4 (Appendix) and visualized in Figure 1 (Appendix). The TDUSW distribution consistently outperforms all rival models across all quantitative indices,

attaining minimal KS, W^*, and A^* distances alongside the largest p-value. Consequently, the model exhibits exceptional flexibility and precision in describing the analyzed COVID-19 mortality data. In addition, the estimated parameters are stable and their corresponding standard errors are relatively small, indicating satisfactory estimation performance for the proposed distribution.

6.2 Application 2

Secondly, the data comprise COVID-19 mortality rates observed in the United Kingdom during a 24-day period starting on October 15, 2020. The observations were collected from the World Health Organization website at https://covid19.who.int/. These values correspond to the recorded daily mortality rates and are listed as follows:

0.2240, 0.2189, 0.2105, 0.2266, 0.0987, 0.1147,
0.3353, 0.2563, 0.2466, 0.2847, 0.2150, 0.1821,
0.1200, 0.4206, 0.3456, 0.3045, 0.2903, 0.3377,
0.1639, 0.1350, 0.3866, 0.4678, 0.3515, 0.3232.

The TDUSW distribution is compared with several competing lifetime distributions using different goodness-of-fit measures, including the Kolmogorov–Smirnov statistic (KS), Cramér–von Mises statistic (W^*), Anderson–Darling statistic (A^*), and the corresponding p-values. The maximum likelihood estimates and their standard errors are also reported. The statistical summary and graphical evaluations for all fitted distributions are detailed in Table 5 (Appendix) and Figure 2 (Appendix), establishing the superior modeling capacity of the TDUSW distribution as validated by minimal KS, W^*, and A^* distances and the highest p-value among all fitted models. Furthermore, the estimated parameters of the TDUSW model are associated with relatively small standard errors, which supports the stability and reliability of the estimation procedure. Hence, the TDUSW distribution can be regarded as an effective model for analyzing COVID-19 mortality rate data.

6.3 Concluding Remarks on the Two Applications

Based on the analysis of the two COVID-19 mortality data sets, the TDUSW distribution showed strong fitting performance when compared with the other considered models. In most situations, the proposed distribution yielded lower values of the KS, W^*, and A^* statistics along with higher corresponding p-values. The graphical tools also supported the numerical outcomes and illustrated the capability of the TDUSW model to describe the data behavior effectively. Therefore, the TDUSW distribution may serve as a useful model for fitting skewed biomedical and reliability data sets.

7 Conclusion

In this study, the TDUSW distribution was introduced as a flexible two-parameter model for analyzing lifetime and skewed data sets. Several statistical properties of the proposed distribution, including the survival function, hazard rate function, quantile function, and moments, were derived.

Different estimation procedures such as MLE, LS, MPS, WLS, CVM, and AD were investigated through simulation analysis. The numerical results showed that the estimators perform efficiently, particularly for large sample sizes.

Finally, two COVID-19 mortality data sets were analyzed to evaluate the practical usefulness of the TDUSW model. The obtained results indicated that the proposed distribution provides a competitive and accurate fit compared with other well-known distributions. The simulation findings are summarized in Table 1 (Appendix), Table 2 (Appendix), and Table 3 (Appendix). These tables provide a detailed comparison of the six estimation methods, namely MLE, LS, MPS, WLS, CVM, and AD, under different parameter configurations and sample sizes. For $n = 25$, the estimates show relatively larger MSE values and greater deviations from the corresponding true parameter values, particularly for the shape parameter α. As the sample size increases to 70 and then to 150, the MSE values decrease markedly for both α and β, while the corresponding mean estimates become progressively closer to their true values. This pattern is observed for all three considered values of α, although the magnitude of the improvement differs among the estimation methods.

For $\alpha = 0.6$ in Table 1 (Appendix), the MLE and MPS procedures generally produce estimates close to the nominal values, with relatively small MSEs across the three sample sizes. A similar improvement is observed for the other methods as the sample size increases. In Table 2 (Appendix), where $\alpha = 1.7$, the same general tendency is maintained, with the estimation errors becoming smaller for larger samples. Table 3 (Appendix), corresponding to $\alpha = 3$, also shows increasing estimation accuracy with increasing sample size. Although the methods do not have identical performance for every parameter configuration, the overall reduction in MSE demonstrates the stabilizing effect of a larger sample size. The results therefore provide numerical evidence that the considered estimation procedures become more reliable as the amount of available information increases.

Table 4 (Appendix) and Table 5 (Appendix) assess the fitted models using two COVID-19 mortality data sets. Table 4 (Appendix) shows that the TDUSW distribution gives the smallest KS statistic (0.1392) and the largest p-value (0.4681) among the considered models. It also has the smallest W^* value (0.1024),

while its A^* value (0.6018) remains competitive. In comparison, several alternative models produce larger KS statistics and much smaller p-values, indicating a less satisfactory representation of the observed data. The MOEx model, for example, has a very large KS statistic and a p-value close to zero, together with relatively large standard errors, suggesting difficulties in obtaining a stable fit.

For the United Kingdom COVID-19 data in Table 5 (Appendix), the TDUSW model again provides the most favorable overall fit. It has the lowest KS statistic (0.0894), the largest p-value (0.9782), and the smallest W^* and A^* values among the fitted models. The competing models show varying levels of fit, with some producing larger KS statistics, smaller p-values, or relatively large standard errors. In particular, the MOEx model exhibits substantial standard errors and a very large KS statistic, indicating considerable estimation and fitting difficulties for this data set. Overall, the results in Table 4 (Appendix) and Table 5 (Appendix) support the flexibility of the TDUSW distribution and its ability to provide an adequate representation of both COVID-19 data sets.

Acknowledgements
The author has no specific acknowledgements to declare.

Declaration of Generative AI and AI-assisted Technologies in the Writing Process

During the preparation of this work, the author(s) utilized artificial intelligence (AI) technologies solely for the purpose of linguistic refinement and grammatical correction. Following the application of these tools, the author(s) comprehensively reviewed, verified, and edited the resulting text. The author(s) maintain full accountability and responsibility for the accuracy, integrity, and final content of the publication.

References:

[1] Gupta, R. D., & Kundu, D. (1999). Theory & Methods: Generalized exponential distributions. *Australian & New Zealand Journal of Statistics*, *41*(2), 173–188. https://doi.org/10.1111/1467-842X.00072

[2] Lee, C., Famoye, F., & Olumolade, O. (2007). Beta-Weibull distribution: Some properties and applications to censored data. *Journal of Modern Applied Statistical Methods*, *6*(1), 173–186. https://doi.org/10.22237/jmasm/1177992960

[3] Weibull, W. (1951). A statistical distribution function of wide applicability. *Journal of Applied Mechanics*, *18*(3), 293–297. https://doi.org/10.1115/1.4010337

[4] Mudholkar, G. S., & Srivastava, D. K. (1993). Exponentiated Weibull family for analyzing bathtub failure-rate data. *IEEE Transactions on Reliability*, *42*(2), 299–302. https://doi.org/10.1109/24.229504

[5] Eugene, N., Lee, C., & Famoye, F. (2002). Beta-normal distribution and its applications. *Communications in Statistics—Theory and Methods*, *31*(4), 497–512. https://doi.org/10.1081/STA-120003130

[6] Cordeiro, G. M., & de Castro, M. (2011). A new family of generalized distributions. *Journal of Statistical Computation and Simulation*, *81*(7), 883–898. https://doi.org/10.1080/00949650903530745

[7] Nadarajah, S., & Kotz, S. (2004). The beta Gumbel distribution. *Mathematical Problems in Engineering*, *2004*(4), 323–332. https://doi.org/10.1155/S1024123X04403068

[8] Alzaatreh, A., Lee, C., & Famoye, F. (2013). A new method for generating families of continuous distributions. *METRON*, *71*(1), 63–79. https://doi.org/10.1007/s40300-013-0007-y

[9] Klein, J. P., & Moeschberger, M. L. (2003). *Survival Analysis: Techniques for Censored and Truncated Data*. Springer New York. ISBN: 9780387216454. https://doi.org/10.1007/b97377

[10] Lawless, J. F. (2002). *Statistical Models and Methods for Lifetime Data* (2nd ed.). Wiley. ISBN: 9781118033005. https://doi.org/10.1002/9781118033005

[11] Xie, M., Tang, Y., & Goh, T. N. (2002). A modified Weibull extension with bathtub-shaped failure rate function. *Reliability Engineering & System Safety*, *76*(3), 279–285. https://doi.org/10.1016/S0951-8320(02)00022-4

[12] Saboor, A., Bakouch, H. S., & Khan, M. N. (2016). Beta Sarhan–Zaindin modified Weibull distribution. *Applied Mathematical Modelling*, *40*(13–14), 6604–6621. https://doi.org/10.1016/j.apm.2016.01.033

[13] Cordeiro, G. M., Ortega, E. M. M., & Nadarajah, S. (2010). The Kumaraswamy Weibull distribution with application to failure data. *Journal of the Franklin Institute*, *347*(8), 1399–1429. https://doi.org/10.1016/j.jfranklin.2010.06.010

[14] Aljarrah, M. A., Lee, C., & Famoye, F. (2014). On generating T-X family of distributions using quantile functions. *Journal of Statistical Distributions and Applications*, *1*, Article 2. https://doi.org/10.1186/2195-5832-1-2

[15] Rezaei, S., Sadr, B. B., Alizadeh, M., & Nadarajah, S. (2017). Topp–Leone generated family of distributions: Properties and applications. *Communications in Statistics—Theory and Methods*, *46*(6), 2893–2909. https://doi.org/10.1080/03610926.2015.1053935

[16] Lemonte, A. J., & Cordeiro, G. M. (2013). An extended Lomax distribution. *Statistics*, *47*(4), 800–816. https://doi.org/10.1080/02331888.2011.568119

[17] Kumar, S. (2020). Monitoring novel corona virus (COVID-19) infections in India by cluster analysis. *Annals of Data Science*, *7*(3), 417–425. https://doi.org/10.1007/s40745-020-00289-7

[18] Lalmuanawma, S., Hussain, J., & Chhakchhuak, L. (2020). Applications of machine learning and artificial intelligence for Covid-19 (SARS-CoV-2) pandemic: A review. *Chaos, Solitons & Fractals*, *139*, 110059. https://doi.org/10.1016/j.chaos.2020.110059

[19] Wáng, Y. X. J. (2020). A call for caution in extrapolating chest CT sensitivity for COVID-19 derived from hospital data to patients among general population. *Quantitative Imaging in Medicine and Surgery*, *10*(3), 798–799. https://doi.org/10.21037/qims.2020.03.04

[20] Bullock, J., Luccioni, A., Pham, K. H., Lam, C. S. N., & Luengo-Oroz, M. (2020). Mapping the landscape of artificial intelligence applications against COVID-19. *Journal of Artificial Intelligence Research*, *69*, 807–845. https://doi.org/10.1613/jair.1.12162

[21] Almetwally, E. M., Alharbi, R., Alnagar, D., & Hafez, E. H. (2021). A new inverted Topp-Leone distribution: Applications to the COVID-19 mortality rate in two different countries. *Axioms*, *10*(1), Article 25. https://doi.org/10.3390/axioms10010025

[22] Jamal, F., Chesneau, C., & Elgarhy, M. (2020). Type II general inverse exponential family of distributions. *Journal of Statistics and Management Systems*, *23*(3), 617–641. https://doi.org/10.1080/09720510.2019.1668159

[23] Almetwally, E. M., & Muhammed, H. Z. (2020). On a bivariate Fréchet distribution. *Journal of Statistics Applications & Probability*, *9*(1), 71–91. https://doi.org/10.18576/jsap/090108

[24] El-Morshedy, M., Alhussain, Z. A., Atta, D., Almetwally, E. M., & Eliwa, M. S. (2020). Bivariate Burr X generator of distributions: Properties and estimation methods with applications to complete and Type-II censored samples. *Mathematics*, *8*(2), Article 264. https://doi.org/10.3390/math8020264

[25] Kim, J. M., Ju, H., & Jung, Y. (2020). Copula approach for developing a biomarker panel for prediction of dengue hemorrhagic fever. *Annals of Data Science*, *7*(4), 697–712. https://doi.org/10.1007/s40745-020-00293-x

Contribution of Individual Authors to the Creation of a Scientific Article (Ghostwriting Policy)

All authors contributed equally to the conceptualization, methodology, software implementation, formal analysis, investigation, writing—original draft preparation, and writing—review and editing of this work. All authors have read and agreed to the published version of the manuscript.

Sources of Funding for Research Presented in a Scientific Article or Scientific Article Itself

No funding was received for conducting this study.

Conflict of Interest

The authors have no conflicts of interest to declare that are relevant to the content of this article.

Creative Commons Attribution License 4.0 (Attribution 4.0 International, CC BY 4.0)

This article is published under the terms of the Creative Commons Attribution License 4.0
https://creativecommons.org/licenses/by/4.0/deed.en_US

APPENDIX

Table 1. Mean estimates and corresponding MSE values for the MLE, LSE, MPSE, WLSE, CVME, and ADE methods for the TDUSW distribution when $\alpha = 0.6$.

β	n	Par.	MLE		LS		MPS		WLS		CVM		AD	
			Mean	MSE	Mean	MSE	Mean	MSE	Mean	MSE	Mean	MSE	Mean	MSE
0.6	25	α	0.5841	0.0149	0.6072	0.0178	0.5838	0.0127	0.6118	0.0158	0.6289	0.0210	0.6140	0.0148
		β	0.6034	0.0189	0.6117	0.0247	0.6032	0.0174	0.6130	0.0225	0.6258	0.0279	0.6141	0.0205
0.6	70	α	0.5922	0.0048	0.6038	0.0059	0.5920	0.0044	0.6059	0.0050	0.6138	0.0064	0.6050	0.0049
		β	0.5998	0.0061	0.6041	0.0078	0.5997	0.0059	0.6048	0.0070	0.6096	0.0082	0.6049	0.0068
0.6	150	α	0.5966	0.0021	0.6019	0.0028	0.5965	0.0020	0.6032	0.0024	0.6061	0.0029	0.6028	0.0023
		β	0.6003	0.0027	0.6025	0.0035	0.6002	0.0026	0.6030	0.0032	0.6044	0.0037	0.6027	0.0031

Source: created by the authors.

Table 2. Mean estimates and corresponding MSE values for the MLE, LSE, MPSE, WLSE, CVME, and ADE methods for the TDUSW distribution when $\alpha = 1.7$.

β	n	Par.	MLE		LS		MPS		WLS		CVM		AD	
			Mean	MSE	Mean	MSE	Mean	MSE	Mean	MSE	Mean	MSE	Mean	MSE
0.6	25	α	1.5856	0.0862	1.6591	0.0890	1.5859	0.0791	1.6831	0.0833	1.7591	0.1119	1.7054	0.0786
		β	0.6037	0.0029	0.6047	0.0032	0.6036	0.0028	0.6059	0.0030	0.6094	0.0034	0.6072	0.0030
1.7	70	α	1.6371	0.0307	1.6867	0.0385	1.6373	0.0308	1.7001	0.0337	1.7221	0.0407	1.7017	0.0324
		β	1.7028	0.0075	1.7042	0.0086	1.7027	0.0074	1.7058	0.0080	1.7089	0.0088	1.7067	0.0080
3	150	α	1.6627	0.0137	1.6982	0.0187	1.6628	0.0142	1.7040	0.0159	1.7147	0.0194	1.7033	0.0152
		β	3.0005	0.0118	3.0028	0.0130	3.0003	0.0117	3.0040	0.0122	3.0066	0.0131	3.0042	0.0122

Source: created by the authors.

Table 3. Mean estimates and corresponding MSE values for the MLE, LSE, MPSE, WLSE, CVME, and ADE methods for the TDUSW distribution when $\alpha = 3$.

β	n	Par.	MLE		LS		MPS		WLS		CVM		AD	
			Mean	MSE	Mean	MSE	Mean	MSE	Mean	MSE	Mean	MSE	Mean	MSE
0.6	25	α	2.8337	0.1408	2.8969	0.1058	2.8339	0.1606	2.9309	0.0985	2.9607	0.0714	2.9618	0.0585
		β	0.5988	0.0009	0.5991	0.0011	0.5988	0.0009	0.5999	0.0010	0.6010	0.0011	0.6005	0.0010
1.7	70	α	2.8962	0.0967	2.9926	0.1139	2.8966	0.0970	3.0082	0.0987	3.0529	0.1203	3.0167	0.1010
		β	1.7005	0.0027	1.7022	0.0030	1.7005	0.0027	1.7028	0.0029	1.7048	0.0031	1.7032	0.0028
3	150	α	2.9351	0.0390	2.9925	0.0530	2.9349	0.0405	3.0076	0.0447	3.0218	0.0546	3.0055	0.0435
		β	2.9967	0.0040	2.9981	0.0044	2.9968	0.0040	2.9991	0.0041	3.0003	0.0044	2.9990	0.0041

Source: created by the authors.

Table 4. MLEs, SEs, KS statistics, p-values, W^* and A^* values for the fitted models based on the COVID-19 data set.

Model	Estimates	SE	KS	p-value	W^*	A^*
TDUSW	$(3.2841,\ 0.7418)$	$(0.3925,\ 0.0317)$	0.1392	0.4681	0.1024	0.6018
MKEx	$(2.3017,\ 0.1928)$	$(0.2811,\ 0.0124)$	0.1715	0.2417	0.2145	1.2847
IW	$(3.0926,\ 21.8841)$	$(0.3478,\ 7.9042)$	0.1768	0.2146	0.2473	1.4632
IR	(8.0174)	(1.2985)	0.2684	0.0091	0.1698	1.0157
IE	(2.9845)	(0.4763)	0.4172	0.0000	0.1211	0.7248
ITL	(1.1269)	(0.1846)	0.4325	0.0000	0.1457	0.8426
MOEx	$(81.2547,\ 1.3984)$	$(37.6482,\ 0.1465)$	0.9628	0.0000	0.3748	2.1075

Source: created by the authors.

Table 5. MLEs, SEs, KS statistics, p-values, W^* and A^* values for the fitted models based on the United Kingdom COVID-19 data set.

Model	Estimates	SE	KS	p-value	W^*	A^*
TDUSW	$(1.4286,\ 11.9043)$	$(0.2481,\ 1.3274)$	0.0894	0.9782	0.0216	0.1588
MKEx	$(2.1068,\ 2.2415)$	$(0.3412,\ 0.1584)$	0.0971	0.9614	0.0268	0.1914
ITL	(20.6185)	(4.1087)	0.2285	0.1263	0.0421	0.2918
IR	(0.0412)	(0.0087)	0.1714	0.4528	0.1496	0.9015
IW	$(2.2419,\ 0.0241)$	$(0.3286,\ 0.0157)$	0.1827	0.3515	0.1635	1.0047
IE	(0.2146)	(0.0428)	0.3624	0.0021	0.0987	0.6452
MOEx	$(48.7715,\ 14.8263)$	$(34.6842,\ 2.4018)$	0.9561	0.0000	0.1142	0.7328

Source: created by the authors.

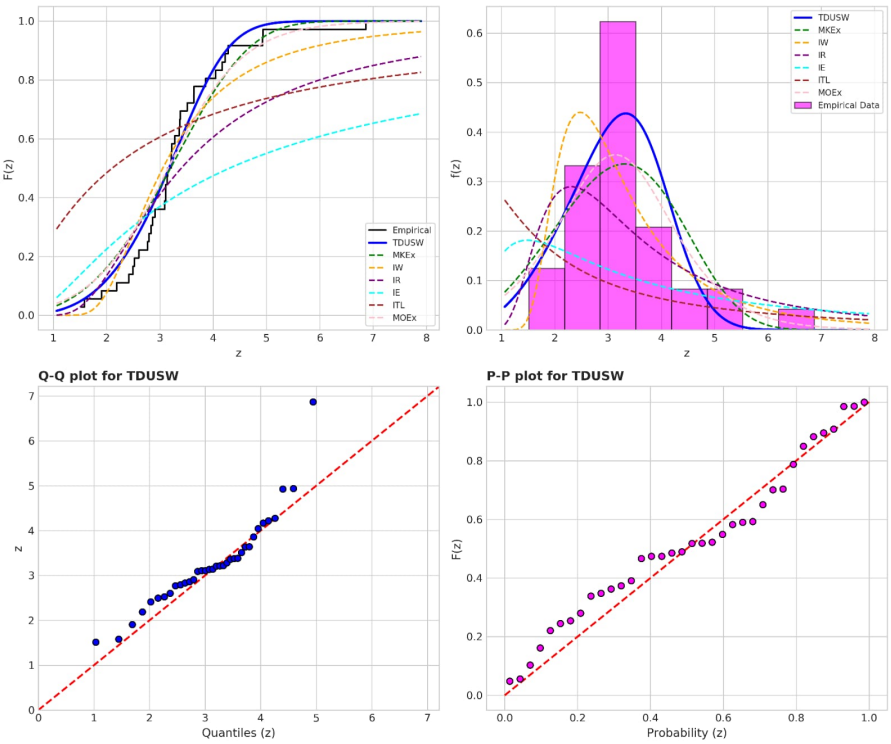

Fig. 1: Graphical assessment of the TDUSW model fitted to the Canadian COVID-19 mortality data using the empirical and fitted CDFs, histogram, Q–Q plot, and P–P plot.

Source: created by the authors.

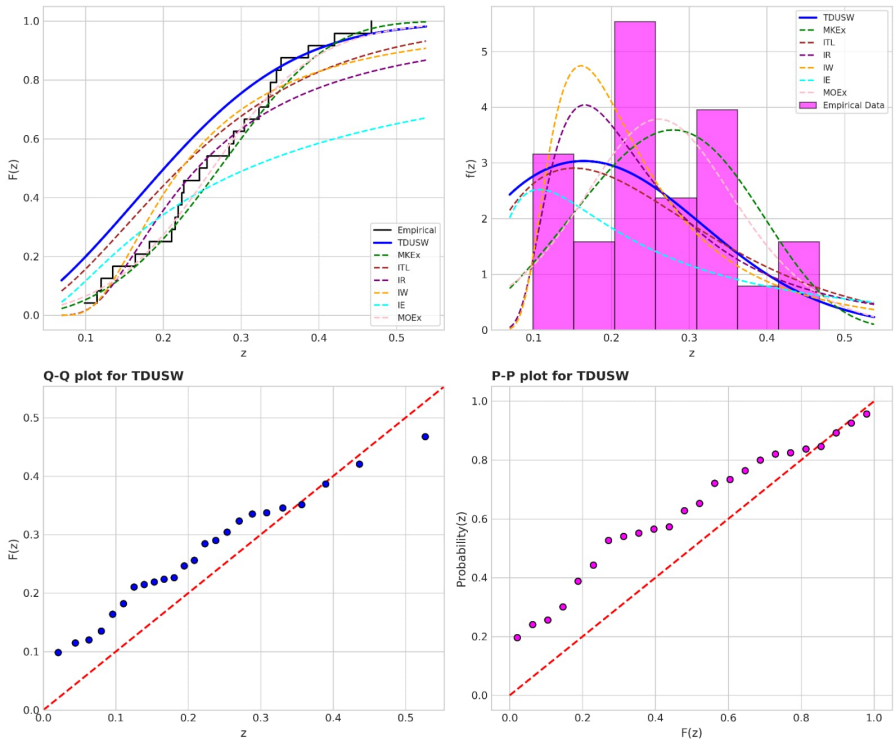

Fig. 2: Graphical assessment of the TDUSW distribution fitted to the UK COVID-19 data using the empirical and fitted CDFs, histogram, Q–Q plot, and P–P plot.

Source: created by the authors.